AMERICAN ACADEMY OF OPHTHALMOLOGY®

The Effect of Pegcetacoplan Treatment on Photoreceptor Maintenance in Geographic Atrophy Monitored by Artificial Intelligence–Based OCT Analysis

Sophie Riedl, MD,[1] Wolf-Dieter Vogl, PhD,[1] Julia Mai, MD,[1] Gregor S. Reiter, MD, PhD,[1] Dmitrii Lachinov, MSc,[1] Christoph Grechenig, MD,[1] Alex McKeown, PhD,[2] Lukas Scheibler, PhD,[2] Hrvoje Bogunović, PhD,[1] Ursula Schmidt-Erfurth, MD[1]

Purpose: To investigate the therapeutic effect of intravitreal pegcetacoplan on the inhibition of photoreceptor (PR) loss and thinning in geographic atrophy (GA) on conventional spectral-domain OCT (SD-OCT) imaging by deep learning–based automated PR quantification.

Design: Post hoc analysis of a prospective, multicenter, randomized, sham (SM)-controlled, masked phase II trial investigating the safety and efficacy of pegcetacoplan for the treatment of GA because of age-related macular degeneration.

Participants: Study eyes of 246 patients, randomized 1:1:1 to monthly (AM), bimonthly (AEOM), and SM treatment.

Methods: We performed fully automated, deep learning–based segmentation of retinal pigment epithelium (RPE) loss and PR thickness on SD-OCT volumes acquired at baseline and months 2, 6, and 12. The difference in the change of PR loss area was compared among the treatment arms. Change in PR thickness adjacent to the GA borders and the entire 20° scanning area was compared between treatment arms.

Main Outcome Measures: Square-root transformed PR loss area in μm or mm, PR thickness in μm, and PR loss/RPE loss ratio.

Results: A total of 31 556 B-scans of 644 SD-OCT volumes of 161 study eyes (AM 52, AEOM 54, SM 56) were evaluated from baseline to month 12. Comparison of the mean change in PR loss area revealed statistically significantly less growth in the AM group at months 2, 6, and 12 than in the SM group (−41 μm ± 219 vs. 77 μm ± 126; $P = 0.0004$; −5 μm ± 221 vs. 156 μm ± 139; $P < 0.0001$; 106 μm ± 400 vs. 283 μm ± 226; $P = 0.0014$). Photoreceptor thinning was significantly reduced under AM treatment compared with SM within the GA junctional zone, as well as throughout the 20° area. A trend toward greater inhibition of PR loss than RPE loss was observed under therapy.

Conclusions: Distinct and reliable quantification of PR loss using deep learning–based algorithms offers an essential tool to evaluate therapeutic efficacy in slowing disease progression. Photoreceptor loss and thinning are reduced by intravitreal complement C3 inhibition. Automated quantification of PR loss/maintenance based on OCT images is an ideal approach to reliably monitor disease activity and therapeutic efficacy in GA management in clinical routine and regulatory trials. *Ophthalmology Retina 2022;6:1009-1018 © 2022 by the American Academy of Ophthalmology. This is an open access article under the CC BY-NC-ND license (http://creativecommons.org/licenses/by-nc-nd/4.0/).*

Supplemental material available at www.ophthalmologyretina.org.

Recently, promising results have been reported from phase II and III trials investigating the safety and efficacy of pegcetacoplan, a complement C3 inhibitor, for the treatment of geographic atrophy (GA). Patients treated with intravitreal pegcetacoplan showed reduced GA progression rates in a dose-dependent manner as assessed by fundus autofluorescence (FAF) imaging.[1,2] GA as the late nonneovascular disease stage of age-related macular degeneration (AMD) causes progressive and irreversible degeneration of choriocapillaris, retinal pigment epithelium (RPE), and photoreceptors (PRs).[3] As central visual function typically remains unaffected until more progressed disease stages reach the fovea,[4] morphological biomarkers are indispensable in monitoring disease activity.

Conventionally, as done in the Study of Pegcetacoplan (APL-2) Therapy in Patients With Geographic

https://doi.org/10.1016/j.oret.2022.05.030
ISSN 2468-6530/22

Atrophy (FILLY) trial, assessment of disease progression has been performed using FAF imaging.[5] This 2-dimensional modality has been the only anatomic primary end point that has so far been accepted by the Food and Drug Administration (FDA) for GA trials, arising from the pre-OCT era.[6,7] Fundus autofluorescence offers robust information only with respect to atrophy of the RPE as a late stage of advanced neurosensory loss. Visualization of PR loss, the condition of the junctional zone, and RPE atrophy within the fovea by FAF imaging does not provide reliable or near as quantifiable information as high-resolution 3-dimensional spectral-domain OCT (SD-OCT). Moreover, FAF image acquisition is not as well established in clinical routine in contrast to SD-OCT, which is currently the most frequently used diagnostic imaging procedure throughout medicine. Spectral-domain OCT enables detailed, cross-sectional visualization of all neurosensory layers, of which the PR layer as the morphological correlate of visual function in particular is of greatest interest. The use of OCT imaging and morphologic analyses have strongly enhanced the in-depth knowledge with respect to the sequence of pathomorphologic events in high-risk intermediate AMD.[8] Furthermore, OCT enables detailed characterization of the so-called junctional zone, an area exhibiting outer retinal changes closely surrounding the GA lesion, revealing PR loss that often exceeds the area of RPE atrophy.[9,10] Pronounced expansion of the RPE-defined GA lesion toward the regions of preceding PR loss has been shown recently.[11,12] These findings highlight the role of primary PR loss in GA and the necessity of reliable PR assessment with accurate quantification to objectively monitor disease progression during the natural course of GA and, more importantly, therapeutic benefits in terms of PR maintenance. Subclinical PR-related features, however, cannot be easily identified or even quantified by human experts in clinical practice. Specifically designed and trained algorithms using artificial intelligence (AI) technology are able to accurately and reliably detect retinal biomarkers such as PR and quantify morphological changes in a fast and automated manner.

In the Study of Pegcetacoplan (APL-2) Therapy in Patients With Geographic Atrophy (FILLY), which is the first to provide proof of principle of C3 inhibition efficacy by FAF grading, we hereby investigate the potential of pegcetacoplan in preventing PR loss and degradation, as assessed by SD-OCT in the original prospective phase II clinical trial data. To further characterize our findings, we assess PR loss and the treatment effect on PR loss in relation to RPE loss, assessed on OCT. To this end, we applied advanced deep learning–based image analysis methods to segment RPE loss and PR layer loss, as well as an alteration in a reliable and reproducible fashion.

Methods

Study Design, Participants, and Study Assessments

This post hoc analysis was performed on the 12-month data of the FILLY trial (ClinicalTrials.gov identifier: NCT02503332), a prospective, multicenter, randomized, masked, sham (SM)-controlled phase II study investigating the safety and efficacy of pegcetacoplan for the treatment of GA. The study design, primary outcomes, and patient demographics have been previously published.[1] Major inclusion criteria for the original trial were a minimum age of 50 years, best-corrected visual acuity of 24 letters or better, and a GA lesion of 2.5 to 17.5 mm^2 (or at least 1 lesion of 1.25 mm^2 or more if multifocal) secondary to AMD confirmed by FAF imaging. The fellow eye was allowed to present GA, neovascular AMD, or both. A total of 246 patients were randomized 1:1:1 to SM, monthly (AM), and bimonthly (AEOM) treatment. OCT volumes were acquired at baseline and months 2, 6, and 12. Using the Spectralis OCT (Heidelberg Engineering), volumes were acquired in the follow-up mode, providing intrapatient registration. Therefore, for this analysis, only patients imaged using the Spectralis OCT were included (79% of participants). Vendor assignment was dependent on the participating study center in the original trial and, thus, was not expected to introduce any bias. The imaging protocol for Spectralis requested 49 B-scans covering the central 20° of the macula.

All patients provided written, informed consent, and institutional review board approval was obtained at participating centers. All study procedures were conducted in accordance with the Declaration of Helsinki. All patient data were fully pseudonymized. Approval for this post hoc analysis was obtained from the Ethics Committee at the Medical University of Vienna.

Image Analysis (PR and RPE Segmentation)

Automated segmentation of PR thickness was performed by a previously reported and extensively evaluated U-Net–based fully convolutional neural network (CNN) delineating the PR layer on each individual B-scan of the entire SD-OCT volume.[13] The segmentation tool captures the area between the top of the ellipsoid zone (EZ) and the outer boundary of the interdigitation zone representative of the core PR anatomy. From the voxel-level binary segmentation, an en face PR thickness map was calculated, providing a thickness value for each single A-scan. In a postprocessing step, EZ loss, henceforth termed PR loss, was defined as an axial PR thickness of ≤ 4 μm. For the purpose of this study, the algorithm was additionally validated in a similar way to Orlando et al[13] by comparing thickness maps in terms of the average thickness of PR, as well as computing segmentation overlap using the metrics Dice coefficient, Precision, and Recall. This was done on a subset of 24 baseline SD-OCT volumes of the FILLY trial. The subset consisted of 6 randomly chosen patients per each of 4 groups, defined by the quantiles of lesion size in the FILLY trial (< 4 mm^2, 4–6.4 mm^2, 6.4–9.8 mm^2, and $> 9.8 mm^2$). Photoreceptor layers were annotated in 5 evenly distributed B-scans per volume in a similar way as published by Orlando et al,[13] namely, by capturing the top of the EZ and the outer boundary of the third hyperreflective outer retinal band. Areas showing RPE loss were excluded from computations, as the main interest of this work lies in areas outside of RPE loss and thickness values are only reported on these areas in the paper, to avoid RPE loss areas with zero PR thickness from dominating the metrics. Performance is presented in the results section.

A separate CNN was specifically trained and validated for detecting RPE loss on OCT, directly translating to the location and size of the clinical appearance of the GA lesion. The architecture of this 3-dimensional–to–2-dimensional CNN is based on an innovative U-shaped architecture that allows to segment a 3-dimensional volume as a 2-dimensional en face binary map reflecting the A-scans with RPE loss.[14] The 3-dimensional–to–2-dimensional CNN was trained on an in-house (Vienna Clinical Trial Center at the

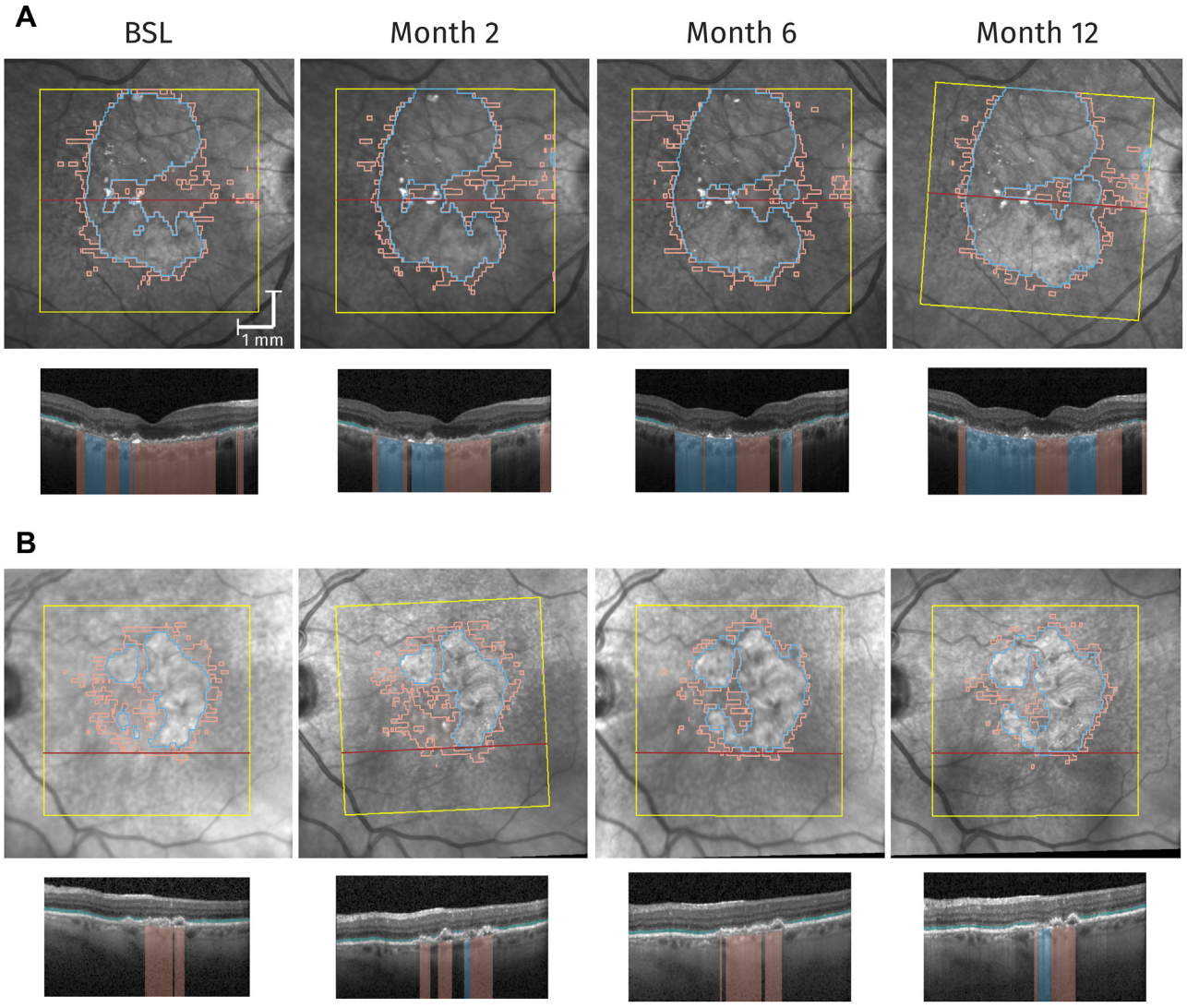

Figure 1. Geographic atrophy growth from baseline (BSL) to month 12 in exemplary patients of the sham treatment (**A**) and monthly pegcetacoplan treatment (AM) (**B**) arms. Retinal pigment epithelium loss (blue) and photoreceptor (PR) loss (red) are shown as en face visualizations (upper rows) and example B-scans (lower rows). Retinal pigment epithelium loss extends into regions of preexisting PR loss, which further increases in (**A**) up to month 12, whereas showing reduced growth under AM treatment (**B**).

Department of Ophthalmology and Optometry, Medical University of Vienna) longitudinal data set, consisting of 192 SD-OCT volumes of 37 patients with GA,[15] using fivefold cross-validation. The trained method was additionally evaluated on an extensive set of reference manual annotations of A-scans with RPE loss, performed on 260 OCT-scans of 147 eyes of the FILLY trial with a total of 12 740 annotated B-scans. Results have been previously published and reflect the high accuracy of the segmentation.[14] The output of such a CNN is a 2-dimensional binary en face map of detected RPE loss, which can be directly brought in correspondence with the en face PR thickness map. Example results of such automated segmentation, registration, and en face visualization are shown in Figure 1.

Statistics

We compared the different aspects of PR quantification between the treatment arms to provide insight into changes located around the GA lesion border, as well as overall PR changes throughout the posterior pole of the individual eyes.

Firstly, the difference in change over time in the PR loss area was compared between treatment arms. In the second analysis, we investigated differences in the change of PR thickness in a predefined 1-mm junctional zone, adjacent to the GA lesion between treatment groups. In addition, we analyzed differences in PR thickness in the entire 20° scanning area. Therefore, the difference between quantitative PR thickness changes over time was compared between treatment arms. To avoid bias by previously analyzed regions with complete PR loss, A-scans showing such complete PR loss either at the respective visit or at year 1 were excluded from this analysis. Thirdly, we compared the ratio of the PR loss area to the RPE loss area between treatment arms at months 2, 6, and 12. To avoid a bias toward smaller ratios because of RPE loss exceeding the borders of the OCT scanning area, square-root transformed lesions of $>$ 3230-µm RPE loss at baseline, equal to the 75% quantile, were excluded from this analysis. A fourth analysis was performed to investigate the differences in growth of RPE loss at year 1 between baseline quartiles of PR loss/RPE loss ratio and the effect of treatment within these quartiles. To

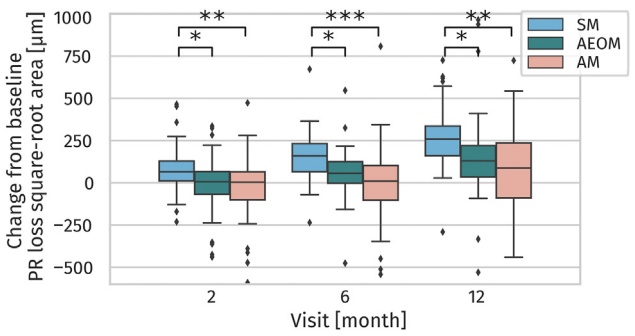

Figure 2. Comparison between change in photoreceptor (PR) loss square-root area in µm from baseline to months 2, 6, and 12 between sham (SM) treatment (blue), every other month (green) and monthly pegcetacoplan treatment (AM) (red) pegcetacoplan treatment groups. Symbol * indicates significance level < 0.05, Symbol ** indicates significance level < 0.01, and symbol *** indicates significance level < 0.001; diamond-shaped symbols represent outliers. AEOM = every other month pegcetacoplan treatment.

this end, a multivariable regression model was calculated considering quartiles of PR loss/RPE loss at baseline and interaction with treatment.

For analyses of RPE and PR loss areas, square-root transformation was applied to account for the dependence of lesion growth on the baseline lesion size. Comparisons of PR thickness and PR loss areas between treatment groups were performed using 1-way analysis of covariance, correcting for respective baseline PR loss area in the latter.

Results

Baseline Data and Lesion Characteristics

Of a total of 246 eyes of 246 patients included in the FILLY trial; 195 eyes of 195 patients were imaged using the Spectralis OCT (Heidelberg Engineering). Data from 34 eyes had to be excluded because of incomplete follow-up. Consequently, our analyses were performed on data of 161 eyes of 161 patients (56 SM, 51 AEOM, 54 AM), imaged at 4 time points, yielding a total of 31 556 B-scans of 644 SD-OCT volumes.

The baseline mean square-root transformed PR loss area did not differ between SM (3.41 mm ± 0.95), AEOM (3.50 mm ± 0.99), and AM (3.37 mm ± 0.82) groups. Likewise, the baseline mean PR thickness in areas that were not affected by PR loss by month 12 did not show any statistically significant difference between SM (24.4 µm ± 3.9), AEOM (22.9 µm ± 5.3), and AM (24.3 µm ± 3.7) groups, respectively.

Performance of the Automated PR Segmentation in an Additional Validation on a Subset of the FILLY trial

The average thickness of the PR layer did not show any statistically significant difference between segmentations provided by manual annotation versus the automated segmentation algorithm (*t* tests: $P = 0.261$; Wilcoxon sign-rank test: $P = 0.177$), indicating that the average thickness estimation is not affected by the automated approach. Furthermore, we report a mean ± standard deviation Dice score of 0.838 ± 0.084, Precision of 0.914 ± 0.058, and Recall of 0.786 ± 0.126, each computed over all eyes. These results are comparable to those reported by Orlando et al.[13] A Bland–Altman plot comparing manual and automated thickness for all 24 cases is shown in Figure S1 (available at www.ophthalmologyretina.org).

PR Loss under Pegcetacoplan Treatment

Figure 2 illustrates the change in PR loss area from baseline to month 12 among the study arms. Numerical results are summarized in Table 1A. The comparison of mean change in PR loss size by months 2, 6, and 12 between AM and SM revealed statistically significantly reduced PR loss in the AM group at all time points, respectively (−41 µm ± 219 vs. 77 µm ± 126; $P = 0.0004$; −5 µm ± 221 vs. 156 µm ± 139; $P < 0.0001$; 106 µm ± 400 vs. 283 µm ± 226; $P = 0.0014$). Change in PR loss size in AEOM-treated patients showed significantly reduced loss compared with SM-treated patients and consistently ranged between values of SM and AM treatment at months 2, 6, and 12 (−8 µm ± 162; $P = 0.013$ vs. SM; 69 µm ± 195; $P = 0.021$ vs. SM; 154 µm ± 249; $P = 0.033$ vs. SM, respectively).

PR Thinning under Pegcetacoplan Treatment

Figure 3 illustrates overall and junctional zone changes of PR thickness; Table 1B and 1C shows full results. Analysis of change in PR thickness was performed in a predefined rim of 1 mm surrounding the RPE atrophy lesion and the overall macular area surrounding this zone. In the junctional zone, statistically significant superior preservation of PR thickness in the AM group compared with SM by month 2 (0.44 µm ± 2.28 vs. −0.57 µm ± 1.59; $P = 0.0072$), month 6 (0.95 µm ± 2.37 vs. −0.59 µm ± 1.40; $P < 0.0001$), and month 12 (0.90µm ± 4.21 vs. −0.95 ± 2.13; $P = 0.0014$) was detected.

Likewise, the comparison of the overall mean change in PR thickness outside of atrophic areas revealed statistically significant less overall PR thinning under both AM and AEOM treatment than SM by month 2 (0.19 µm ± 1.72 and −0.010 µm ± 1.84 vs. −0.95 µm ± 2.13; $P = 0.0067$ and $P = 0.052$), month 6 (0.87 µm ± 1.59 and 0.15 µm ± 2.28 vs. −1.31 µm ± 3.03; both $P < 0.0001$), and month 12 (0.73 µm ± 2.70 and −0.12 µm ± 2.11 vs. −2.28 µm ± 3.25; both $P < 0.0001$).

Differential Effect of Pegcetacoplan Treatment on PR Loss versus RPE Loss

Assessing the ratio of PR loss area to RPE loss area over time allows differentiation of the treatment effect on different morphologic layers and corresponding cell types. A trend of treatment to maintain PR integrity to a higher extent than RPE integrity was observed. Although the PR/RPE loss ratio remained stable throughout baseline and months 2, 6, and 12 in patients of the SM group (1.25 ± 0.20, 1.24 ± 0.21, 1.23 ± 0.19, 1.23 ± 0.19, respectively), it was gradually reduced under AEOM (1.36 ± 0.33, 1.30 ± 0.26, 1.29 ± 0.25, 1.28 ± 0.25) and AM treatment with pegcetacoplan (1.32 ± 0.25, 1.28 ± 0.18, 1.26 ± 0.19, 1.22 ± 0.15), respectively. However, there was no statistically significant difference of PR/RPE loss ratio changes between treatment groups at months 2, 6, or 12 (AEOM vs. SM: $P = 0.263$; $P = 0.247$; $P = 0.687$; AM vs. SM: $P = 0.272$; $P = 0.566$; $P = 0.138$, respectively).

Table 1. Comparison of the Change in Photoreceptor Loss (A) and Thickness (B and C) from Baseline to Months 2, 6, and 12 between Patients Receiving SM, AEOM, and AM Pegcetacoplan Treatment

	Mean ± SD PR Loss Area (Square-Root Transformed) [µm]				
A.	SM	AEOM	AM	***P* Value AEOM vs. SM**	***P* Value AM vs. SM**
Baseline	3408 ± 949	3501 ± 994	3366 ± 824	0.606	0.810
Change month 2 to BSL	77 ± 126	−8 ± 162	−41 ± 219	**0.013**	**0.0004**
Change month 6 to BSL	156 ± 139	69 ± 195	−5 ± 221	**0.021**	**< 0.0001**
Change month 12 to BSL	283 ± 226	154 ± 249	106 ± 400	**0.033**	**0.0014**
	Mean ± SD PR Thickness [µm] in the 1-mm Border Zone				
B.	SM	AEOM	AM	***P* Value AEOM vs. SM**	***P* Value AM vs. SM**
Baseline	16.6 ± 6.8	15.7 ± 7.7	16.6 ± 6.2	0.485	0.974
Change month 2 to BSL	−0.57 ± 1.59	0.11 ± 1.94	0.44 ± 2.28	0.090	**0.0072**
Change month 6 to BSL	−0.59 ± 1.40	0.15 ± 1.68	0.95 ± 2.37	0.053	**< 0.0001**
Change month 12 to BSL	−0.95 ± 2.13	−0.04 ± 2.16	0.90 ± 4.21	0.14	**0.0014**
	Mean ± SD PR Thickness [µm] in the 6 × 6 Macular Area				
C.	SM	AEOM	AM	***P* Value AEOM vs. SM**	***P* Value AM vs. SM**
Baseline	24.4 ± 3.9	22.9 ± 5.3	24.3 ± 3.7	0.084	0.95
Change month 2 to BSL	−0.95 ± 2.82	−0.010 ± 1.84	0.19 ± 1.72	0.052	**0.0067**
Change month 6 to BSL	−1.31 ± 3.03	0.15 ± 2.28	0.87 ± 1.59	**0.0036**	**< 0.0001**
Change month 12 to BSL	−2.28 ± 3.25	−0.12 ± 2.11	0.73 ± 2.70	**< 0.0001**	**< 0.0001**

AEOM = every other month pegcetacoplan treatment; AM = monthly pegcetacoplan treatment; BSL = baseline; PR = photoreceptor; SD = standard deviation; SM = sham.
Bold values indicate statistical significance level below 0.05.

Effect of Baseline PR Loss/RPE Loss Ratio on RPE Loss Growth under Treatment

Distribution of eyes based on PR loss/RPE loss quartiles between treatment arms is shown in Table 2A, and results of modeling growth of RPE loss, as well as treatment effect thereon, depending on PR loss/RPE loss ratio are shown in Table 2B and Figure 4. Geographic atrophy growth in SM-treated eyes increased with higher baseline PR loss/RPE loss ratio quartiles. Lesions in the highest quartile showed statistically significantly increased growth of RPE loss of 284 µm (95% confidence interval [CI], 84–485; $P = 0.006$) compared with lesions in the lowest

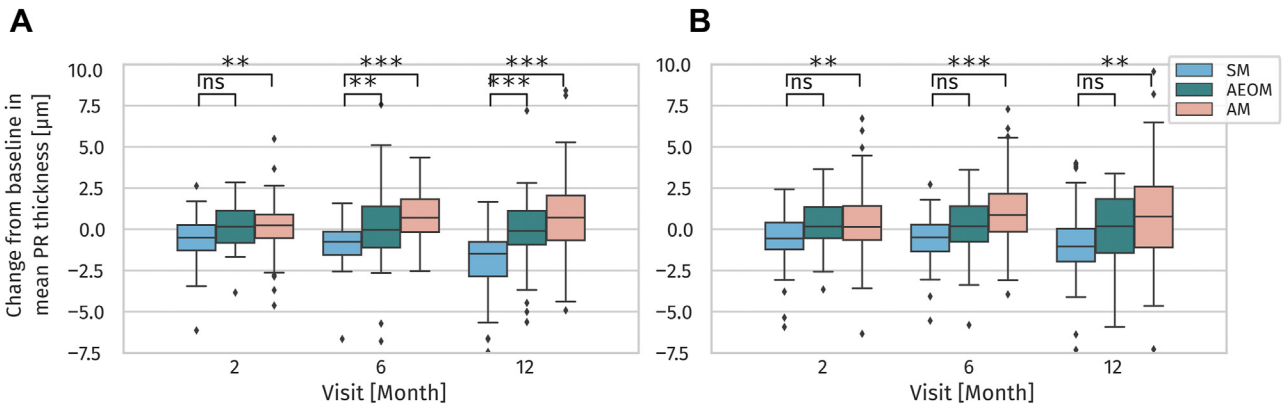

Figure 3. Comparison between change in mean photoreceptor (PR) thickness in µm from baseline to months 2, 6, and 12 in the 20° scanning region outside of atrophic areas (**A**) and in a 1-mm junctional zone adjacent to the retinal pigment epithelium loss lesion (**B**) between sham (SM) treatment (blue), every other month (green) and monthly pegcetacoplan treatment (AM) (red) pegcetacoplan treatment groups. Symbol ** indicates significance level < 0.01, and symbol *** indicates significance level < 0.001; diamond-shaped symbols represent outliers. AEOM = every other month pegcetacoplan treatment; ns = nonsignificant.

Table 2. Count of Eyes per Baseline Quartile of PR Loss/RPE Loss Ratio and Treatment Group Are Listed in (A). (B) Multivariable Regression Model of RPE Square-Root Area Change Between Baseline and 1 Year Considering Quartiles of PR Loss/RPE Loss Ratio and Interaction* with Treatment

	Number of Eyes		
A. PR Loss/RPE Loss Quartile	SM	AEOM	AM
1	13	10	8
2	10	10	10
3	10	7	13
4	6	11	13

B.	Value (µm)	95% CI	*P* Value
Intercept	203	90 to 314	**< 0.001**
PR loss/RPE loss quartile			**0.036**
1	—	—	
2	66	−105 to 237	0.45
3	151	−20 to 322	0.083
4	284	84 to 485	**0.006**
PR loss/RPE loss quartile * treatment			0.52
1 * AEOM	−7.4	−178 to 164	0.93
2 * AEOM	−61	−243 to 121	0.51
3 * AEOM	−89	−290 to 111	0.38
4 * AEOM	−49	−255 to 157	0.64
1 * AM	−8.6	−191 to 174	0.93
2 * AM	−59	−241 to 123	0.52
3 * AM	−70	−241 to 102	0.42
4 * AM	−207	−408 to −6.5	**0.043**

AEOM = every other month pegcetacoplan treatment; AM = monthly pegcetacoplan treatment; CI = confidence interval; PR = photoreceptor; RPE = retinal pigment epithelium; SM = sham.
Global *P* values (0.036 and 0.52) over all quartiles are determined by type III analysis of variance. Bold values indicate statistical significance level below 0.05.
*Interaction between PR loss/RPE loss ratio and treatment.

quartile. Likewise, the effect of AM treatment increased with higher PR loss/RPE loss ratio quartiles, reaching a statistically significant effect of −207 µm (95% CI, −408 to −6,5; $P = 0.043$) compared with SM-treated eyes in the fourth quartile.

Discussion

This work for the first time presents an AI-based morphologic analysis of the efficacy of complement C3 inhibition in GA. The condition of PRs is reported with high precision, including analyses of both PR loss and thinning. We thereby provide objective proof of principle that complement inhibition can indeed preserve PRs as the major correlate of retinal function.

In GA, central best-corrected visual acuity typically remains unimpaired until advanced disease destroys central regions of the macula. Moreover, once the central island is lost, the best-corrected visual acuity will not further correlate with lesion growth. Alternative measurements of visual function, such as microperimetry, that do highlight functional abnormalities relevant to the patient's visual performance, such as parafoveal scotomas, have so far been restricted to research settings. Standardization between patients and different manufacturers constitutes a substantial difficulty including the extensive variability of psychophysical measurements between individuals.[16] A large spectrum of patient-reported outcome measures has been applied in GA disease with inferior outcomes compared with anatomic end points regarding reliability, specificity, and sensitivity.[17] Therefore, clinicians and regulators concluded that a distinction between disease progression and consequently therapeutic efficiency cannot be made clinically without morphologic guidance. OCT-based measurements of GA lesions have been shown to correlate with

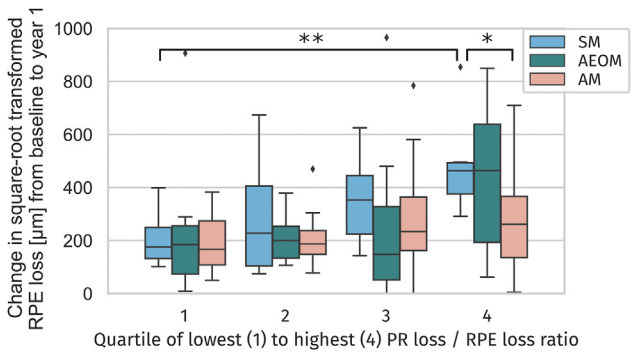

Figure 4. Comparison of retinal pigment epithelium (RPE) loss growth from baseline to year 1 between quartiles of baseline photoreceptor (PR)/RPE loss ratio in sham (SM) treatment (blue), every other month (green), and monthly pegcetacoplan treatment (AM) (red)—treated eyes. Symbol * indicates significance level < 0.05, and symbol ** indicates significance level < 0.01; diamond-shaped symbols represent outliers. AEOM = every other month pegcetacoplan treatment.

gold-standard FAF measurements,[10,18] also in the setting of pegcetacoplan treatment.[19] Undoubtedly, OCT offers more detailed information targeting the affected layers, specifically the outer retinal bands attributed to PR anatomy. Robust correlations of PR loss on OCT with functional loss[20,21] and local GA progression[11,12] have led to the recommendation of morphologic monitoring of GA in both clinical practice and standardized clinical trials. This notion has clearly been supported by a National Eye Institute and FDA end points workshop on AMD in 2017, which concluded that "prevention of PR loss as seen on OCT might be considered a potential trial end point in atrophic AMD given the established link between PR loss and visual function."[22] Following comparable reports on excellent structure−function correlation in macular telangiectasia type 2,[23,24] the area of EZ loss has been defined as the primary outcome measure in a randomized SM-controlled phase II trial evaluating the effect of treatment with ciliary neurotrophic factor.[25] Therefore, PR loss defined on SD-OCT was rated of higher importance than the functional measures, which were ranged as secondary outcome parameters.

An increasing spectrum of novel therapeutic options for degenerative macular disease are expected in the short-to-midterm future.[26] With innovative therapeutic strategies comes a high demand for precise and reproducible morphologic monitoring of PR loss/maintenance, and a paradigm-shifting solution is demonstrated in our current study: The volumetric nature of OCT data allows for precise quantification beyond mere 2-dimensional en face representations such as FAF imaging. However, the level of precision and reproducibility required for the identification of subtle features on a micron-scale can hardly be reached and maintained by human image graders not even considering the challenge of busy clinical practices with GA being 4 times more frequent than neovascular AMD, which already presents an overwhelming burden to health care professionals.[27] Just in recent years, the introduction of AI into ophthalmic image analyses has led to huge advances in the field of medical retina, predominantly with respect to structure−function correlation, as well as treatment monitoring and prediction of neovascular AMD, but also in the field of morphology-based risk stratification of intermediate AMD and GA.[28−32] In the same National Eye Institute/FDA workshop mentioned above, it was noted that "the more automated the measurements, the greater the likelihood of precision and accuracy."[15] The results of AI-based measurements as demonstrated in our pilot study are highly accurate and consistent over time and treatment adjudication. This robustness is a result of comprehensive training and validation in as many as 12 740 B-scans of 260 SD-OCT volumes.

Specifically, PR thinning on OCT has been shown to be an early atrophic sign for high-risk intermediate AMD.[8] The ability of our AI-based tool to capture not only complete loss but also incomplete damage adds to the benefit of AI-based image reading. Particularly in GA, where an established loss of neurosensory structures cannot be reversed, intervention should be performed at the earliest time of alteration, supposing that it can be objectively detected. Identification of early signs of neurodegeneration will also be crucial for the prediction of progression in GA patients discriminating slow from fast progressors regarding follow-up intervals and therapeutic regimens.

The presented analysis widely expands on our pathophysiological knowledge derived from AI-based analysis of subclinical features, and this objectively confirms the benefit of C3 inhibitory pegcetacoplan treatment of GA in respect of PR maintenance and halting progression of GA. Complement activation by oxidative stress has long been identified as a major pathogenetic component and potential therapeutic target in AMD. Nevertheless, several previous attempts of using complement inhibitors have failed in clinical trials for GA.[33,34] The FILLY trial, investigating the efficacy of intravitreal C3 inhibition, was the first to report success in slowing GA growth in a phase II and recently phase III trial.[1,2] Immunohistochemistry of nonhuman primates has identified the choriocapillaris as the main location of C3 presentation.[35] Correspondingly, the choriocapillaris is one of the most relevant locations of disease manifestation in GA and has been suspected as the site of disease initiation.[36] However, functional loss occurs because of PR degradation. Our analyses reveal both PR loss and PR thinning to be slowed in pegcetacoplan-treated patients. Evidence of C3 deposition on PRs activating glial cells such as macrophages, which has been shown to lead to their degradation by activation of the complement cascade,[35] substantiates an effect of pegcetacoplan on the level of the PRs. Patients treated with pegcetacoplan even presented with a mean decrease in PR loss area at months 2 and 6. This might be explained by the shifting of recovered PRs, which has been reported experimentally after destruction with selective laser photocoagulation,[37] but is also expected to reflect measurement inaccuracies, as discussed within the limitations section.

Furthermore, we observed a trend toward a higher decrease in the PR loss/RPE loss ratio during follow-up, which might indicate pegcetacoplan to slow PR loss to a greater extent than RPE loss. In addition to EZ loss as a known marker of PR degradation, we also report specifically on thinning of the EZ, which has been previously shown to be an early atrophic sign.[8] Analogous to PR loss, we even observed a mean increase in PR thickness in pegcetacoplan-treated patients. However, the precise morphologic correlate remains unclear. Remodeling changes, as well as measurement inaccuracies, may contribute to this effect. Importantly, the PR-preserving effect of treatment, shown by both markers, was evident in a dose-dependent manner. A subanalysis on RPE loss growth and treatment effect depending on PR loss/RPE loss ratio provided 2 relevant findings. Firstly, it confirmed PR loss exceeding the GA lesion to be a driver of faster RPE loss growth in SM-treated eyes, which has been shown in previous investigations.[11,12] Secondly, we observed the treatment effect to be PR loss/RPE loss ratio-dependent, showing a significant RPE loss growth reduction for AM compared with SM-treated eyes in the highest ratio quartile. These results highlight the importance of baseline characteristics for investigating treatment effects and are expected

to be of relevance for defining criteria with respect to patient selection for forthcoming clinical trials. Furthermore, future treatment guidelines might be based on lesion characteristics such as PR loss/RPE loss ratio because of the reported difference in treatment effect.

The deduction of the clinical relevance of our presented morphologic analyses is not straightforward. Our results entail large CIs, calling for cautious interpretation. However, the fact that CIs present almost consistently larger in treated compared with untreated patients indicates the range in treatment response that contributes to data variance, which in turn highlights the need for morphology-based patient selection. Also, the interpretation of the PR thickness results will require future investigations on functional correlations. From a morphologic point of view, the difference in PR thinning averaged over large areas between SM and AM-treated patients of almost 2 μm (junctional zone) and 3 μm (overall macular area) after 12 months of treatment is comparable to what we have seen occur within 1 year in patients with high-risk intermediate AMD[8] and can be assumed to be of clinical relevance.

Limitations of this analysis include possible errors in our automated segmentation method. Previous and also additional validations, presented within this paper, show reliable quantification of PR thickness with no statistically significant difference between automated and manually generated results. Nevertheless, outliers, which are not expected to influence the overall signal of our analyses, may occur. Furthermore, minor shifts of 1 B-scan at follow-up are inevitable despite image registration. However, these are expected to be distributed randomly throughout the entire patient cohort. By selecting only patients imaged by Spectralis OCT, which provides excellent visualization of the PR bands, we aimed to minimize segmentation-based bias. Despite robust structure—function correlation for the EZ, functioning PR cells might be present despite their loss on OCT because of directionality-dependent reflectivity, and—vice-versa—function may be lost despite PR presence on OCT imaging. Such discrepancies cannot be entirely ruled out in a morphology-based analysis. Ultimately, it should be noted that our study presents an exploratory and not statistically predetermined analysis of a potentially nonrandom subset of OCT data.

In summary, this is the first report on AI-based morphologic analysis of the effect of complement inhibition on PR preservation in patients with GA. This comes with 2 important implications. First, the results are expected to support the regulatory approval process of a breakthrough treatment strategy, which is urgently needed to prevent severe visual loss in the largest population of AMD patients in line with the statement that, "given the variability in measuring visual function, the FDA agency is willing to consider anatomic end points."[22] Second, the specification of OCT as an appropriate imaging modality and PRs as the target biomarker has opened the doors for advanced therapeutic developments in a visionary manner. The report stated further that "if PR loss can be prevented at least to the extent to the fuzzy border, as seen on OCT, around the GA lesion, that might be considered a potential trial end point."[22] Our work provides such evidence. With respect to evidence-based selection of patients with high chances to profit from treatment, the learning process has just begun and will undoubtedly require further investigations on the functional relevance of morphologic changes, also incorporating patient-reported outcomes. The other major implication is the availability of a fast and accurate monitoring strategy, which can provide a reliable and user-friendly decision support tool into the hands of retina experts and general ophthalmologists having to manage larger AMD populations by intravitreal injections than ever before, as soon as the novel therapies become available. We anticipate that health care providers will appreciate the quality of AI-based patient selection and treatment guidance. Our promising results highlight the vital need for the retina community to effectively monitor GA in an evidence-based and morphologic manner.

Footnotes and Disclosures

Originally received: February 14, 2022.
Final revision: April 28, 2022.
Accepted: May 27, 2022.
Available online: June 3, 2022. Manuscript no. ORET-D-22-00115R1.

[1] OPTIMA - Laboratory for Ophthalmic Image Analysis, Department of Ophthalmology and Optometry, Medical University of Vienna, Vienna, Austria.

[2] Apellis Pharmaceuticals Inc, Waltham, Massachusetts.

Presented at the Annual Meeting of the Association of Research in Vision and Ophthalmology 2021.

Disclosure(s):

All authors have completed and submitted the ICMJE disclosures form.

The author(s) have made the following disclosure(s): A.M.K.: Employee — Apellis Pharmaceuticals.

L.S.: Employee — Apellis Pharmaceuticals.

H.B.: Research grant — Apellis Pharmaceuticals.

U.S.E.: Scientific Consultancy — Genentech, Novartis, Roche, Heidelberg Engineering, Kodiak, RetInSight.

The FILLY Phase 2 study was conducted by Apellis Pharmaceuticals and our work was in part supported by an Apellis research grant. The financial support by the Austrian Federal Ministry for Digital and Economic Affairs and the National Foundation for Research, Technology and Development is gratefully acknowledged. The funding organizations had no role in the design and conduct of this research.

HUMAN SUBJECTS: Human subjects were included in this study. All patients provided written, informed consent and institutional review board approval was obtained at participating centers. All study procedures were conducted in accordance with the Declaration of Helsinki. All patient data was fully pseudonymized. Approval for this post hoc analysis was obtained from the Ethics Committee at the Medical University of Vienna.

No animal subjects were used in this study.

Author Contributions:

Conception and design: Riedl, Vogl, Mai, Reiter, Bogunović, Schmidt-Erfurth

Data collection: Riedl, Vogl, Lachinov, Grechenig, McKeown, Scheibler, Bogunović

Analysis and interpretation: Riedl, Vogl, Mai, Reiter, Lachinov, Grechenig, McKeown, Scheibler, Bogunović, Schmidt-Erfurth

Obtained funding: Bogunović

Overall responsibility: Riedl, Vogl, Bogunović, Schmidt-Erfurth

Abbreviations and Acronyms:
AEOM = bimonthly pegcetacoplan treatment; **AI** = artificial intelligence; **AM** = monthly pegcetacoplan treatment; **AMD** = age-related macular degeneration; **CI** = confidence interval; **CNN** = convolutional neural network; **EZ** = ellipsoid zone; **FAF** = fundus autofluorescence; **FDA** = Food and Drug Administration; **FILLY** = Study of Pegcetacoplan (APL-2) Therapy in Patients With Geographic Atrophy; **GA** = geographic atrophy; **PR** = photoreceptor; **RPE** = retinal pigment epithelium; **SD-OCT** = spectral domain OCT; **SM** = sham treatment.

Keywords:
Automated image analysis, Complement inhibition, Geographic atrophy, Optical coherence tomography, Photoreceptors.

Correspondence:
Ursula Schmidt-Erfurth, MD, Spitalgasse 23, 1090 Vienna, Austria. E-mail: ursula.schmidt-erfurth@meduniwien.ac.at.

References

1. Liao DS, Grossi FV, El Mehdi D, et al. Complement C3 inhibitor pegcetacoplan for geographic atrophy secondary to age-related macular degeneration: a randomized phase 2 trial. *Ophthalmology*. 2020;127:186−195.
2. Heier J, Wykoff C, Singh R, et al. Efficacy of intravitreal pegcetacoplan in geographic atrophy: results from the DERBY and OAKS trials. Presentation at the Retina Society 2021, Chicago, USA.
3. Holz FG, Strauss EC, Schmitz-Valckenberg S, van Lookeren Campagne M. Geographic atrophy: clinical features and potential therapeutic approaches. *Ophthalmology*. 2014;121:1079−1091.
4. Sayegh RG, Sacu S, Dunavölgyi R, et al. Geographic atrophy and foveal-sparing changes related to visual acuity in patients with dry age-related macular degeneration over time. *Am J Ophthalmol*. 2017;179:118−128.
5. von Rückmann A, Fitzke FW, Bird AC. Fundus autofluorescence in age-related macular disease imaged with a laser scanning ophthalmoscope. *Invest Ophthalmol Vis Sci*. 1997;38:478−486.
6. Chong V. Endpoints: the beginning of a new treatment? *Ophthalmologica*. 2021;244:365−367.
7. IvericBio. Iveric Bio Receives FDA Agreement Under Special Protocol Assessment (SPA) for GATHER2 Phase 3 Clinical Trial of Zimura® in Geographic Atrophy Secondary to Age-Related Macular Degeneration [Press release]. 2021.
8. Reiter GS, Riedl S, Rivail A, et al. Identification of initial events leading to outer retinal atrophy in age-related macular degeneration using deep learning quanitifications. *ARVO Annual Meeting Presentation*. 2021.
9. Qu J, Velaga SB, Hariri AH, et al. Classification and quantitative analysis of geographic atrophy junctional zone using spectral domain optical coherence tomography. *Retina*. 2018;38:1456−1463.
10. Sayegh RG, Simader C, Scheschy U, et al. A systematic comparison of spectral-domain optical coherence tomography and fundus autofluorescence in patients with geographic atrophy. *Ophthalmology*. 2011;118:1844−1851.
11. Reiter GS, Told R, Schranz M, et al. Subretinal drusenoid deposits and photoreceptor loss detecting global and local progression of geographic atrophy by SD-OCT imaging. *Invest Ophthalmol Vis Sci*. 2020;61:11.
12. Pfau M, von der Emde L, de Sisternes L, et al. Progression of photoreceptor degeneration in geographic atrophy secondary to age-related macular degeneration. *JAMA Ophthalmol*. 2020;138:1026−1034.
13. Orlando JI, Gerendas BS, Riedl S, et al. Automated quantification of photoreceptor alteration in macular disease using optical coherence tomography and deep learning. *Sci Rep*. 2020;10:5619.
14. Lachinov D, Seeböck P, Mai J, et al. *Projective Skip-Connections for Segmentation Along a Subset of Dimensions in Retinal OCT*. Cham: Springer International Publishing; 2021:431−441.
15. Bui PTA, Reiter GS, Fabianska M, et al. Fundus autofluorescence and optical coherence tomography biomarkers associated with the progression of geographic atrophy secondary to age-related macular degeneration. *Eye (Lond)*. 2021. https://doi.org/10.1038/s41433-021-01747-z.
16. Csaky KG, Patel PJ, Sepah YJ, et al. Microperimetry for geographic atrophy secondary to age-related macular degeneration. *Surv Ophthalmol*. 2019;64:353−364.
17. Sadda SR, Chakravarthy U, Birch DG, et al. Clinical endpoints for the study of geographic atrophy secondary to age-related macular degeneration. *Retina*. 2016;36:1806−1822.
18. Velaga SB, Nittala MG, Hariri A, Sadda SR. Correlation between fundus autofluorescence and en face OCT measurements of geographic atrophy. *Ophthalmol Retina*. 2022. https://doi.org/10.1016/j.oret.2022.03.017. In press. https://www.ophthalmologyretina.org/article/S2468-6530(22)00132-4/fulltext
19. Mai J, Lachinov D, Riedl S, et al. GA area measured by SD-OCT shows good correspondence with FAF-based measurements in patients enrolled in the FILLY trial. ARVO 2022 Annual Meeting, Denver, May 1−4 2022.
20. Landa G, Su E, Garcia PM, Seiple WH, Rosen RB. Inner segment-outer segment junctional layer integrity and corresponding retinal sensitivity in dry and wet forms of age-related macular degeneration. *Retina*. 2011;31:364−370.
21. Querques L, Querques G, Forte R, Souied EH. Microperimetric correlations of autofluorescence and optical coherence tomography imaging in dry age-related macular degeneration. *Am J Ophthalmol*. 2012;153:1110−1115.
22. Csaky K, Ferris III F, Chew EY, et al. Report from the NEI/FDA endpoints workshop on age-related macular degeneration and inherited retinal diseases. *Invest Ophthalmol Vis Sci*. 2017;58:3456−3463.
23. Sallo FB, Leung I, Clemons TE, et al. Correlation of structural and functional outcome measures in a phase one trial of ciliary neurotrophic factor in type 2 idiopathic macular telangiectasia. *Retina*. 2018;38:S27−S32.
24. Heeren TFC, Kitka D, Florea D, et al. Longitudinal correlation of ellipsoid zone loss and functional loss in macular telangiectasia type 2. *Retina*. 2018;38:S20−S26.
25. Chew EY, Clemons TE, Jaffe GJ, et al. Effect of ciliary neurotrophic factor on retinal neurodegeneration in patients with macular telangiectasia type 2: a randomized clinical trial. *Ophthalmology*. 2019;126:540−549.

26. Cabral de Guimaraes TA, Daich VM, Georgiou M, Michaelides M. Treatments for dry age-related macular degeneration: therapeutic avenues, clinical trials and future directions. *Br J Ophthalmol*. 2021;106:297−304.
27. Klein R, Klein BE, Knudtson MD, et al. Fifteen-year cumulative incidence of age-related macular degeneration: the Beaver Dam Eye Study. *Ophthalmology*. 2007;114:253−262.
28. Schmidt-Erfurth U, Reiter GS, Riedl S, et al. AI-based monitoring of retinal fluid in disease activity and under therapy. *Prog Retin Eye Res*. 2022;86:100972.
29. Schmidt-Erfurth U, Sadeghipour A, Gerendas BS, et al. Artificial intelligence in retina. *Prog Retin Eye Res*. 2018;67:1−29.
30. Waldstein SM, Vogl WD, Bogunovic H, et al. Characterization of drusen and hyperreflective foci as biomarkers for disease progression in age-related macular degeneration using artificial intelligence in optical coherence tomography. *JAMA Ophthalmol*. 2020;138:740−747.
31. Schmidt-Erfurth U, Bogunovic H, Grechenig C, et al. Role of deep learning-quantified hyperreflective foci for the prediction of geographic atrophy progression. *Am J Ophthalmol*. 2020;216:257−270.
32. Riedl S, Cooney L, Grechenig C, et al. Topographic analysis of photoreceptor loss correlated with disease morphology in neovascular age-related macular degeneration. *Retina*. 2020;40:2148−2157.
33. Holz FG, Sadda SR, Busbee B, et al. Efficacy and safety of lampalizumab for geographic atrophy due to age-related macular degeneration: chroma and spectri phase 3 randomized clinical trials. *JAMA Ophthalmol*. 2018;136:666−677.
34. Yehoshua Z, de Amorim Garcia Filho CA, Nunes RP, et al. Systemic complement inhibition with eculizumab for geographic atrophy in age-related macular degeneration: the COMPLETE study. *Ophthalmology*. 2014;121:693−701.
35. Kim BJ, Mastellos DC, Li Y, Dunaief JL, Lambris JD. Targeting complement components C3 and C5 for the retina: key concepts and lingering questions. *Prog Retin Eye Res*. 2021;83:100936.
36. Scharf J, Corradetti G, Corvi F, et al. Optical coherence tomography angiography of the choriocapillaris in age-related macular degeneration. *J Clin Med*. 2021:10.
37. Sher A, Jones BW, Huie P, et al. Restoration of retinal structure and function after selective photocoagulation. *J Neurosci*. 2013;33:6800−6808.

Pictures & Perspectives

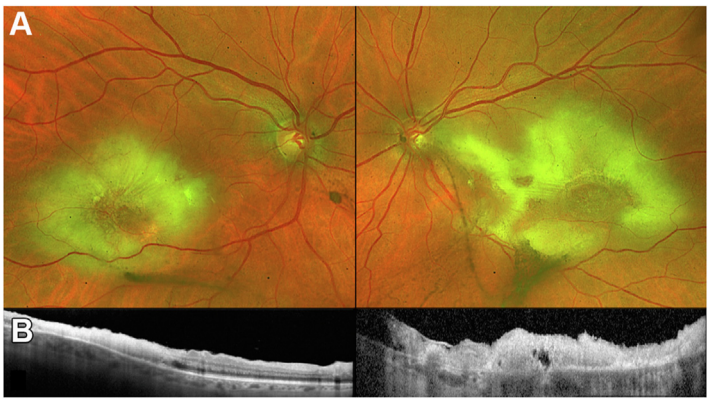

Bilateral Macular Toxoplasmosis

A 78-year-old woman with rheumatoid arthritis, on rituximab, presented with blurry vision and was found to have bilateral vitritis and macular infiltrates without prior chorioretinal scars (Fig **A**). OCT showed bilateral full-thickness macular retinitis (Fig **B**). Serologic testing showed normal *Toxoplasma gondii* immunoglobulin M and mildly elevated immunoglobulin G. Intravitreal foscarnet had no effect. Vitreous fluid polymerase chain reaction test result was negative for herpes simplex virus, varicella−zoster virus, and cytomegalovirus but positive for *T. gondii*. She received intravitreal clindamycin with consolidation of the lesions. This case illustrates the complexity of serologic testing in primary toxoplasmosis retinitis and the importance of its consideration in immunocompromised patients despite normal immunoglobulin M. (Magnified version of Fig **A-B** is available online at www.ophthalmologyretina.org).

Ogul E. Uner, MD
Phoebe Lin, MD, PhD

Department of Ophthalmology, Casey Eye Institute, Oregon Health and Science University, Portland, Oregon